Supporting Information:

Preparation of Graphene-like Iron Oxide Nanofilms/Silica Composite with Enhanced Adsorption and Efficient Photocatalytic Properties

Xiulin Yang,[†,‡] Xueyun Wang,[†,‡] Xianzong Liu,[†] Yanjun Zhang,[†] Weiguo Song,[†] Chunying Shu,[†] Li Jiang*[†] and Chunru Wang*[†]

[†] Beijing National Laboratory for Molecular Sciences, Institute of Chemistry, Chinese Academy of Sciences, Beijing 100190

[‡] University of Chinese Academy of Sciences, Beijing 100039, China

Experimental Section

Materials: All chemical reagents used in this experiment were of analytical grade. $Pb(NO_3)_2$, Methylene blue (MB), tetraethylorthosilicate (TEOS), (3-aminopropyl) triethoxysilane (APTES), Hexadecyl trimethyl ammonium Bromide (CTAB), $FeSO_4 \cdot 7H_2O$, K_2CO_3, HCl, NaOH, ethanol and ethylene glycol were procured commercially and were used as received without further purification.

Preparation of aminated silica **(SiO_2-NH_2).** In a typical synthesis, 4 mL (28 wt%) of $NH_3 \cdot H_2O$ was dissolved into 100 mL of ethanol and 8 mL deionized water under magnetic stirring. After stirring for 15 min, 6 mL of tetraethylorthosilicate (TEOS) was added into the above-prepared mixture with vigorous stirring at 30 °C for 6 h to yield uniform silica spheres. Next, 1.45 mL of (3-aminopropyl) triethoxysilane (APTES) was added into the colloidal solution containing silica spheres and allowed to react for 1 h. The resulting aminated silica was collected by using a PTFE membrane with 0.22 μm pore-size and washed with double-distilled water and ethanol several times, and dried at 70 °C overnight under a vacuum.

Synthesis of graphene-like Fe_2O_3 doped SiO_2-NH_2 **(G-Fe_2O_3/SiO_2-NH_2).** SiO_2-NH_2 (0.1 g, 1.67 mmol), $FeSO_4 \cdot 7H_2O$ (0.1668 g, 0.6 mmol), CTAB (0.2187 g, 0.6 mmol) and K_2CO_3 (0.1658 g, 1.2 mmol) were one-pot dissolved in 60 mL of ethylene glycol (EG)-H_2O (2:1, v/v ratio) mixture. The resultant mixture was ultrasonic vibrations for 30 min and then transferred to a Teflon lined stainless-steel autoclave (capacity of 100 mL). The autoclave was sealed and maintained at 180 °C for 8 h. The system was then cooled to ambient temperature naturally. The final product was collected by using a PTFE membrane with 0.22 μm pore-size and washed with

double-distilled water and ethanol several times, followed by vacuum-drying at 70 °C for 12 h.

Adsorption Experiments. The solution containing different concentrations of Pb(II) and MB with 10, 20, 30, 50, 80 and 100 mg·L^{-1} were prepared using $Pb(NO_3)_2$ and MB as the sources, respectively. The pH value of the MB solution was adjusted to 6.5 with dilute HCl and NaOH solution prior to the adsorption experiments. The time-dependant curves were preformed with the initial concentration for 10 and 20 mg·L^{-1}, and the sample dose is 0.2 g·L^{-1}. At predetermined time intervals, 8 mL supernatant solution of Pb(II) was pipetted and filtered through 0.22 μm PTFE membranes. For the MB, 4 mL analytical samples were taken from the suspension and immediately centrifuged at 10000 rpm for 2 min.

For the adsorption isotherms, 5 mg of the G-Fe_2O_3/SiO_2-NH_2 was added to 25 mL of the above solution under stirring at room temperature. After 12 h, the sample for adsorbed heavy metal ions were separated through 0.22 μm PTFE membrane and analyzed by inductively coupled plasma-optical emission spectroscopy (Shimazu, ICPE-9000) to measure the concentration of metal ions in the remaining solution, and for the MB, 4 mL analytical samples were taken from the suspension and immediately centrifuged at 10000 rpm for 2 min. The adsorption capacity of the adsorbents was calculated according to the following equation:[1]

$$q_e = \frac{(C_0 - C_e)V}{m} \quad (1)$$

where C_0 and C_e represent the initial and equilibrium concentrations (mg·L^{-1}), respectively. V is the volume of the solution (mL), and m is the amount of adsorbent (mg).

***Photodegradation of methyl blue* (MB).** The Fenton oxidation of MB was conducted in a glass beaker with continuous magnetic stirring at room temperature. Before the experiment, the beaker containing 100 mL of 20 mg·L^{-1} MB solution and 20 mg G-Fe_2O_3/SiO_2-NH_2 were stirred in a dark chamber for 30 min to reach the adsorption-desorption equilibrium. Then, 1 mL H_2O_2 (30%, w/w) was injected into the above solution under the irradiation of visible light (Mejiro genossen, MVL-210). At the given time intervals, analytical samples were taken from the suspension and immediately centrifuged at 10000 rpm for 2 min. The MB concentration was measured by using a UV-vis spectrophotometer.

Characterization. The morphology and microstructures of the samples were characterized by field emission scanning electron microscopy (FE-SEM, JEOL 6701F), and transmission electron

microscopy (TEM, JEOL 2010). X-ray diffraction (XRD) patterns were preformed on a Rigaku D/max-2500 diffractometer with Cu Kα radiation (λ = 1.5418 Å) at 40 kV and 30 mA. XPS data were obtained with an ESCALab220i-XL electron spectrometer from VG Scientific using 300W Al K*α* radiation. Fourier transforms infrared spectrometry (FT-IR, Thermo Fisher Scientific) was employed to analyze the surface chemical composition. UV-visible spectroscopy (Shimadzu UV-2550) was used to analyze the concentration of MB at room temperature from 400 to 800 nm. Thermal gravity measurement was made on a TGA/STA409 PC module with a rising temperature rate of 10 °C·min^{-1} from 50 to 1000 °C under continuous N_2 flow. The specific surface areas of the as-prepared products were measured on a Quantachrome Autosorb AS-1 instrument, and the pore size distributions were derived from the desorption branches of the isotherm with the Barrett-Joyner-Halenda (BJH) model. The pH value was measured using pH meter (Thermo Scientific, Model: 410p-13).

Figure Captions

Fig. S1 Transmission electron microscopy images of SiO_2-NH_2.

Fig. S2 EDX analysis of Fe_2O_3/SiO_2-NH_2.

Fig. S3 The BJH pore-size distribution curves of G-Fe_2O_3/SiO_2-NH_2 and SiO_2-NH_2 composites.

Fig. S4 UV–vis absorption spectra of the MB with 10 and 20 mg·L^{-1}.

Fig. S5 Change in aqueous Pb(II) and MB concentration with time. The initial concentrations of Pb(II) is 10 mg·L^{-1} and MB is 10 and 20 mg·L^{-1}. Sample dose is 20 mg/100 mL.

Fig. S6 Adsorption kinetics based on the (A) pseudo-first-order kinetic model and (B) pseudo-second-order kinetic model on the adsorption of MB and Pb(II) ions onto the G-Fe_2O_3/SiO_2-NH_2, the initial concentration is 10 or 20 mg·L^{-1} and sample dose is 20 mg/100 mL.

Fig. S7 Freundlich isotherms model of G-Fe_2O_3/SiO_2-NH_2 adsorbed MB and Pb(II). The initial concentration is 10~100 mg·L^{-1} and sample dose is 5 mg/25 mL.

Fig. S8 The saturated adsorption capacities of G-Fe_2O_3/SiO_2-NH_2 and SiO_2-NH_2 for Pb(II) and MB under the same conditions.

Table S1. Summary of Pb(II) and MB maximum adsorption capacities (q_m) on various adsorbents.

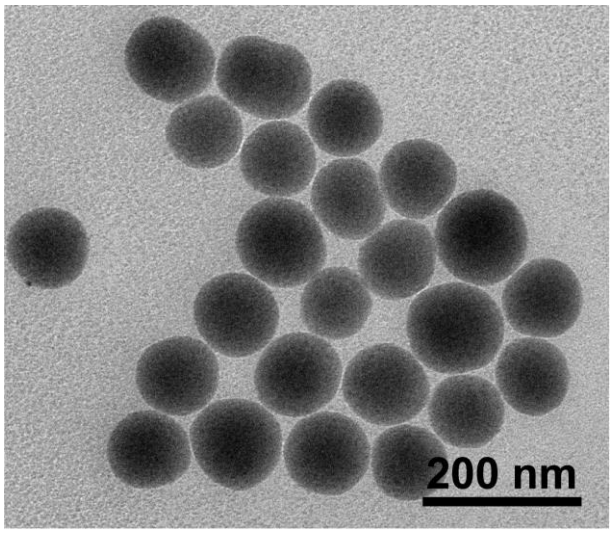

Fig. S1 Transmission electron microscopy images of SiO_2-NH_2.

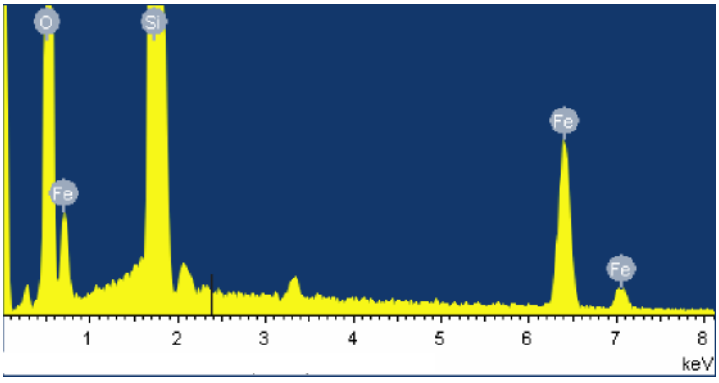

Fig. S2 EDX analysis of G-Fe_2O_3/SiO_2-NH_2.

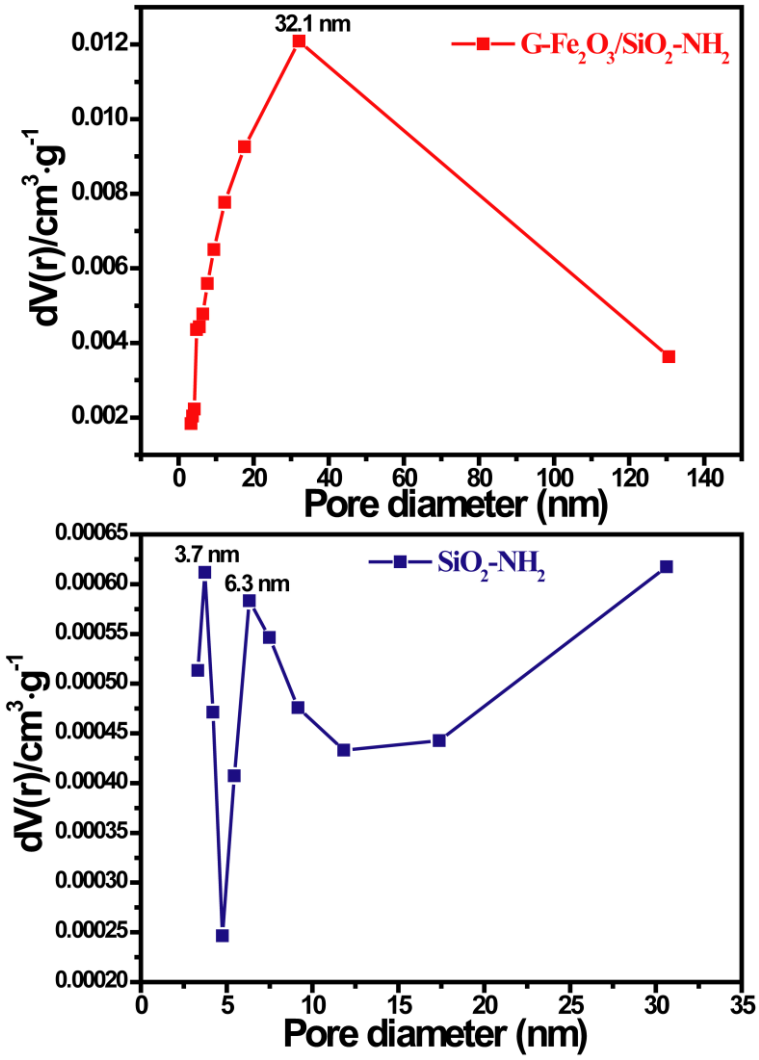

Fig. S3 The BJH pore-size distribution curves of G-Fe_2O_3/SiO_2-NH_2 and SiO_2-NH_2 composites.

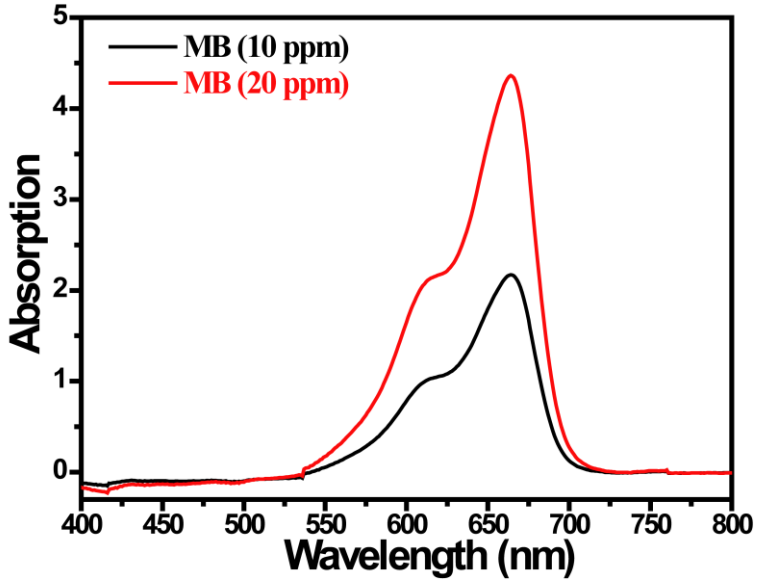

Fig. S4 UV–vis absorption spectra of the MB with 10 and 20 mg·L^{-1}.

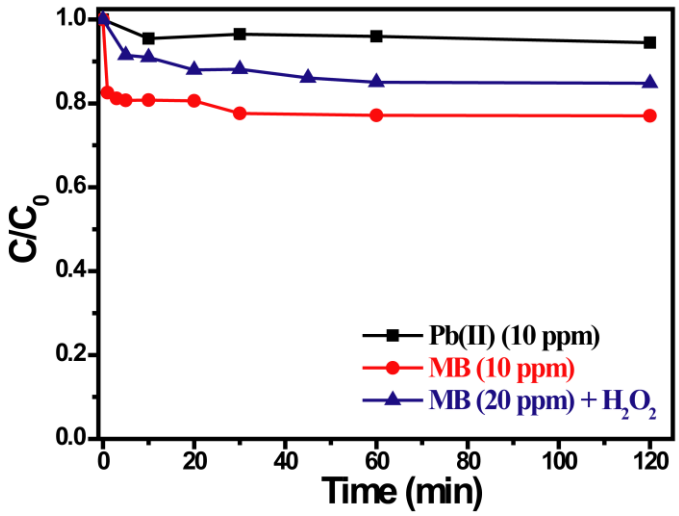

Fig. S5 Change in aqueous Pb(II) and MB concentration with time. The initial concentrations of Pb(II) is 10 mg·L^{-1} and MB is 10 and 20 mg·L^{-1}. Sample dose is 20 mg/100 mL.

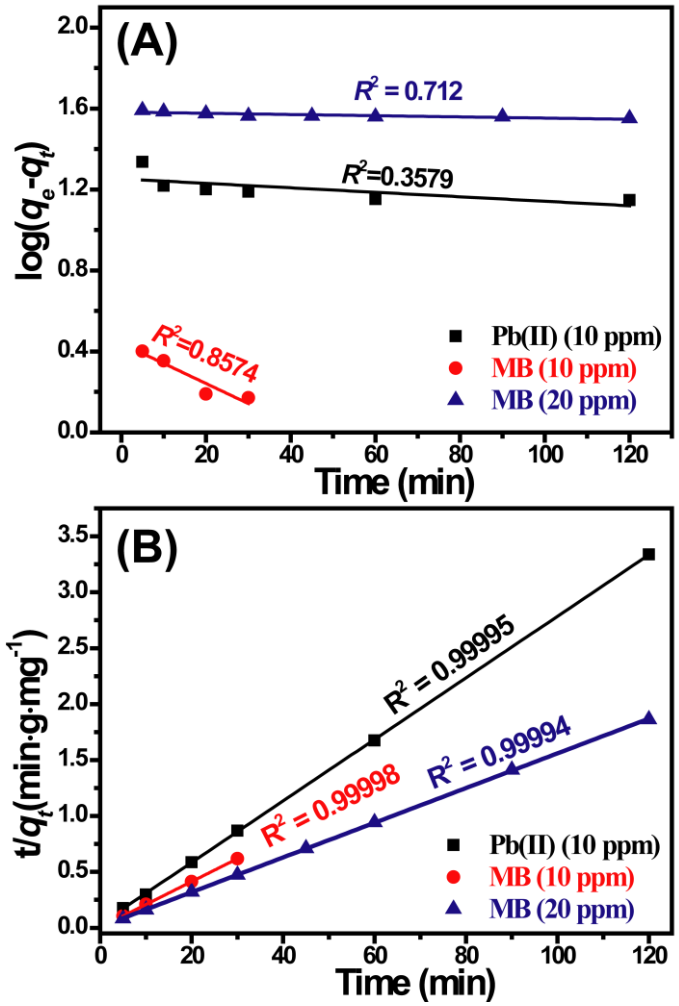

Fig. S6 Adsorption kinetics based on the (A) pseudo-first-order kinetic model and (B) pseudo-second-order kinetic model on the adsorption of MB and Pb(II) ions onto the G-Fe_2O_3/SiO_2-NH_2, the initial concentration is 10 or 20 mg·L^{-1} and sample dose is 0.2 g·L^{-1}.

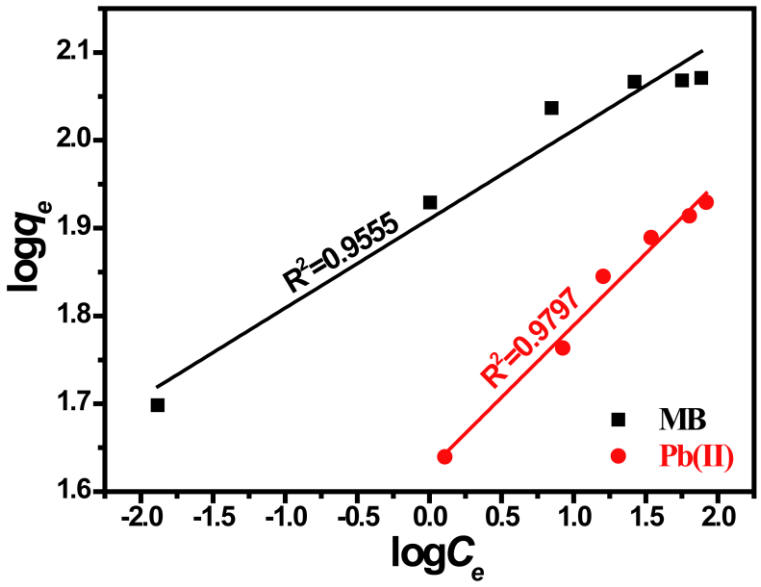

Fig. S7 Freundlich isotherms model of G-Fe_2O_3/SiO_2-NH_2 adsorbed MB and Pb(II). The initial concentration is 10~100 mg·L^{-1} and sample dose is 5 mg/25 mL.

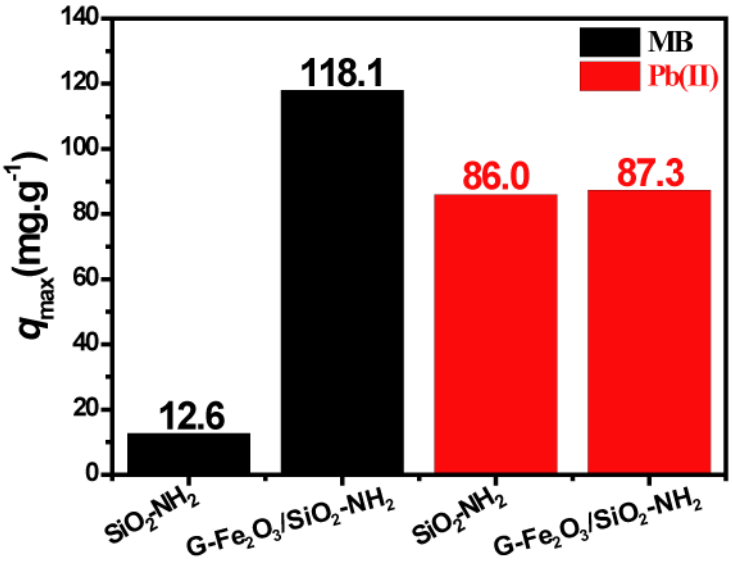

Fig. S8 The saturated adsorption capacities of G-Fe_2O_3/SiO_2-NH_2 and SiO_2-NH_2 for Pb(II) and MB under the same conditions.

Table S1. Summary of Pb(II) and MB maximum adsorption capacities (q_m) on various adsorbents.

Sorbents	Pb(II): q_m ($mg.g^{-1}$)	MB: q_m ($mg.g^{-1}$)	BET ($m^2.g^{-1}$)
G-Fe_2O_3/SiO_2-NH_2 (this study)	87.3	118.1	104.6
Mg-doped Fe_2O_3–ferrihydrite powder [2]	99.1	--	--
Fe_2O_3@Al(OH)CO_3 [3]	89.2	--	320.8
Urchin-like α-FeOOH hollow spheres [4]	80	--	96.9
Magnesium Silicate Hollow Nanostructures [5]	64.79	--	355.21
APAN Nanofiber Mats [6]	60.6	--	--
Manganese oxide-coated bentonite [7]	58.88	--	--
Multiwall carbon nanotubes/iron oxides [8]	37.64		90.68
Magnetic cellulose–chitosan hydrogels [9]	28.1	--	--
Polyacrylonitrile/Silica Nanospheres [10]	22.38	--	--
Honeycomb-like Ni@C composite [11]	21.4	--	29.43
Ceria Hollow Nanospheres [12]	9.2	--	72
Poly(acrylamide) [13]	6.0	--	--
Fe_3O_4/SiO_2-GO nanoparticles [14]	--	97.0	--
Iron Oxide Nanoparticles/Activated Carbon [15]	--	47.62	--
Carbon nanotubes [16]	--	46.2	--
Iron oxide-coated zeolite [17]	--	12.52	--
Coir pith carbon [18]	--	5.87	--

Reference

1 (a) X.-Y. Yu, R.-X. Xu, C. Gao, T. Luo, Y. Jia, J.-H. Liu and X.-J. Huang, *ACS Appl. Mat. Interfaces*, 2012, **4**, 1954-1962; (b) V. Rocher, J.-M. Siaugue, V. Cabuil and A. Bee, *Water Res.*, 2008, **42**, 1290-1298.

2 M. Mohapatra, L. Mohapatra, D. Hariprasad, S. Anand and B. K. Mishra, *Environ. Technol.*, 2011, **33**, 1717-1726.

3 X. Yang, X. Wang, Y. Feng, G. Zhang, T. Wang, W. Song, C. Shu, L. Jiang and C. Wang, *J. Mater. Chem. A*, 2013, **1**, 473-477.

4 B. Wang, H. Wu, L. Yu, R. Xu, T. T. Lim and X. W. Lou, *Adv. Mater.*, 2012, **24**, 1111-1116.

5 Y. Zhuang, Y. Yang, G. Xiang and X. Wang, *J. Phys. Chem. C*, 2009, **113**, 10441-10445.

6 P. Kampalanonwat and P. Supaphol, *ACS Appl. Mat. Interfaces*, 2010, **2**, 3619-3627.

7 E. Eren, B. Afsin and Y. Onal, *J. Hazard. Mater.*, 2009, **161**, 677-685.

8 L. Ji, L. Zhou, X. Bai, Y. Shao, G. Zhao, Y. Qu, C. Wang and Y. Li, *J. Mater. Chem.*, 2012, **22**, 15853-15862.

9 Z. Liu, H. Wang, C. Liu, Y. Jiang, G. Yu, X. Mu and X. Wang, *Chem. Commun.*, 2012, **48**, 7350-7352.

10 Q. Zhao and T. Cao, *Ind. Eng. Chem. Res.*, 2012, **51**, 4952-4957.

11 Y. Ni, L. Jin, L. Zhang and J. Hong, *J. Mater. Chem.*, 2010, **20**, 6430-6436.

12 C.-Y. Cao, Z.-M. Cui, C.-Q. Chen, W.-G. Song and W. Cai, *J. Phys. Chem. C*, 2010, **114**, 9865-9870.

13 V. Mishra and R. Kumar, *J. Appl. Polym. Sci.*, 2013, **128**, 3295-3307.

14 Y. Yao, S. Miao, S. Yu, L. Ping Ma, H. Sun and S. Wang, *J. Colloid Interface Sci.*, 2012, **379**, 20-26.

15 B. Zargar, H. Parham and M. Rezazade, *J. Chin. Chem. Soc.*, 2011, **58**, 694-699.

16 Y. Yao, F. Xu, M. Chen, Z. Xu and Z. Zhu, *Bioresour. Technol.*, 2010, **101**, 3040-3046.

17 L. Zhao, W. Zou, L. Zou, X. He, J. Song and R. Han, *Desalin. Water Treat.*, 2010, **22**, 258-264.

18 D. Kavitha and C. Namasivayam, *Bioresour. Technol.*, 2007, **98**, 14-21.